DEUTSCHES ELEKTRONEN – SYNCHROTRON DESY

DESY 87-135
MZ-TH/87-16
October 1987

EXCLUSIVE SEMI-LEPTONIC DECAYS OF BOTTOM MESONS IN THE SPECTATOR QUARK MODEL

by

J.G. Körner

Institut f. Physik, Johannes-Gutenberg-Universität, Mainz

and

Deutsches Elektronen-Synchrotron DESY, Hamburg

G.A. Schuler

Deutsches Elektronen-Synchrotron DESY, Hamburg

ISSN 0418-9833

NOTKESTRASSE 85 · 2 HAMBURG 52

To be sure that your preprints are promptly included in the
HIGH ENERGY PHYSICS INDEX,
send them to the following address (if possible by air mail):

DESY
Bibliothek
Notkestrasse 85
2 Hamburg 52
Germany

DESY 87-135
MZ-TH/87-16
October 1987

ISSN 0418-9833

EXCLUSIVE SEMI-LEPTONIC DECAYS OF BOTTOM MESONS IN THE SPECTATOR QUARK MODEL

J.G. Körner
Institut für Physik, Joh. Gutenberg-Universität, 6500 Mainz
and
Deutsches Elektronen Synchroton DESY, 2000 Hamburg

G.A. Schuler
Deutsches Elektronen Synchroton DESY, 2000 Hamburg, West Germany

Abstract:

We calculate the exclusive semileptonic bottom meson decays $B \to D(D^*)+\ell^-+\bar{\nu}_\ell$ in the spectator quark model. The helicity structure of the mesonic current transitions $B \to D(D^*)$ is matched to the helicity structure of the free quark current transitions $b \to c$ at minimum momentum transfer $q^2 = 0$. The results are continued to $q^2 = 0$ by pole-dominated form factors. Our results are compared to recent calculations that use quark model dynamics at maximum momentum transfer $q^2_{max} = (M_1-M_2)^2$. We find agreement at q^2_{max}. At $q^2 = 0$ there are significant differences between the predictions of the two approaches leading to marked differences in the predictions for the shape of the lepton energy spectrum, the shape of the q^2-distribution, and the helicity composition of the transition measurable in the angular distributions of the decays $D^* \to D\pi$ and $W^-_{virtual} \to \ell^-+\bar{\nu}_\ell$.

The study of the semileptonic decays of bottom mesons is presently an area of intensive experimental [1] and theoretical work [2-12]. Experimentally, semileptonic $b \to c$ transitions appear to be dominated (~(80-90)%) by the exclusive modes $B \to D(D^*) + \ell^- + \bar{\nu}_\ell$. It is therefore important and worthwhile to develop and experimentally test theoretical models for these two exclusive semileptonic modes.

At present, the main interest in model descriptions of $B \to D(D^*)$ semileptonic decays centers on the interpretation of the lepton energy endpoint spectrum in terms of the strengths of $b \to c$ and $b \to u$ transitions. Needless to say that, apart from settling this important issue, the structure of the $B \to D(D^*)$ semileptonic decays is interesting in its own right, since the decays allow one to study the underlying quark dynamics as probed by the fundamental vector and axial vector currents.

In this paper we develop an approach to the exclusive semileptonic $B \to D(D^*)$ decays where the helicity structure of the semileptonic $B \to D(D^*)$ decays is matched to the helicity structure of the semileptonic $b \to c$ free quark decay at minimum momentum transfer $q^2 = 0$. The results are then continued to $q^2 \neq 0$ via power behaved invariant form factors whose power behaviour is determined by the canonical QCD power counting rules.

This approach is in contrast to recent approaches [5,9] which use the quark model at maximum momentum transfer $q^2_{max} = (M_1-M_2)^2$, where the $D(D^*)$ is produced at rest in the bottom meson rest system. Although our results and the results of [5,9] essentially agree at q^2_{max}, they deviate considerably at $q^2 = 0$. It is clear that any difference in the theoretical input $B \to D(D^*)$ form factor values has important ramifications for the determination of the V_{bc} and V_{bu} Kobayashi-Maskawa matrix elements as extracted from semileptonic bottom meson decay.

Let us begin by defining invariant form factors by (see e.g. [13])

$$\langle D(p_2)|V_\mu|B(p_1)\rangle = F_+^V(p_1+p_2)_\mu$$
$$\langle D^*(p_2)|A_\mu+V_\mu|B(p_1)\rangle = e^*_{2\nu}(F_1^A g_\mu^\nu + F_2^A p_{1\mu} p_1^\nu + iF^V \epsilon_{\mu\nu\rho\sigma} p_1^\rho p_2^\sigma) \qquad (1)$$

In the following we shall always work in the zero-lepton-mass limit. Thus we have dropped invariants multiplying $q_\mu = (p_1-p_2)_\mu$ in (1).*)

In order to fix the $q^2 = 0$ values of the form factors we match the spin properties of the $B \to D$ and $B \to D^*$ transitions to the free quark decay $b \to c$ transitions. The assumption is that the spectator quark is spin-inert. It neither affects the spin properties of the active quarks in the current induced heavy quark to light quark transitions nor is its own spin flipped. To this end we first calculate the free quark decay (FQD) helicity amplitudes h_λ^{FQD} in the heavy quark (m_1) rest system with the light quark (m_2) moving along z. One finds (helicity label is that of the current)

$$h_o^{FQD} = \langle c\uparrow|J_o|b\uparrow\rangle = -(\sqrt{Q_+} + \sqrt{Q_-})\,(p+q_o)/\sqrt{q^2}$$
$$h_o'^{FQD} = \langle c\uparrow|J_o|b\uparrow\rangle = (\sqrt{Q_+} - \sqrt{Q_-})\,\sqrt{q^2}/(p+q_o) \qquad (2)$$
$$h_-^{FQD} = \langle c\uparrow|J_-|b\uparrow\rangle = \sqrt{2}\,(\sqrt{Q_+} + \sqrt{Q_-})$$
$$h_+^{FQD} = \langle c\uparrow|J_+|b\uparrow\rangle = \sqrt{2}\,(\sqrt{Q_+} - \sqrt{Q_-})$$

where $Q_\pm = (m_1 \pm m_2)^2 - q^2$, p is the c.m. momentum $2m_1 p = \sqrt{Q_+ Q_-}$ and q_o is the energy of the virtual W in the c.m. system $q_o = (m_1^2 - m_2^2 + q^2)/2m_1$.

*) Such an approximation would no longer be justified for semileptonic b-decays involving τ-leptons. In this case also the invariants multiplying q_μ would have to be included. It would be interesting to also test our spectator model approach in these decays.

To leading order in m_1 and for small $\sqrt{q^2}$ ($\sqrt{q^2} < m_2 < m_1$) one finds that the longitudinal amplitude $h_o^{FQD} = \langle c\uparrow|J_o|b\downarrow\rangle$ dominates. The transverse (-) helicity amplitude $h_-^{FQD} = \langle c\uparrow|J_-|b\downarrow\rangle$ is down by the helicity flip factor $\sqrt{2q^2}/m_1$ and the transverse (+) helicity amplitude $h_+^{FQD} = \langle c\uparrow|J_+|b\uparrow\rangle$ is down by the helicity suppression factor m_2/m_1 in addition to the helicity flip factor $\sqrt{2q^2}/m_1$. The contribution of the second longitudinal helicity amplitude $h_o'^{FQD} = \langle c\uparrow|J_o|b\uparrow\rangle$ is insignificant in this limit since it is suppressed by $(m_2/m_1)(q^2/m_1^2)$.

For the matching procedure we also need the helicity form factors of the mesonic transitions [13]. They are (helicity label is that of the current)

$$H_o^D = \frac{p}{\sqrt{q^2}}\,2M_1\,F_+^V$$
$$H_o^{D^*} = \frac{1}{2M_2\sqrt{q^2}}\,((M_1^2 - M_2^2 - q^2)\,F_1^A + 2M_1^2 p^2 F_2^A) \qquad (3)$$
$$H_\pm^{D^*} = F_1^A \pm M_1 p F^V$$

We use the minimum momentum transfer point $q^2 = 0$ to do the matching. At $q^2 = 0$ one is far enough away from the problematic region $q^2_{max} = (M_1 - M_2)^2$ where the (pseudo-) threshold behaviour of the various spin transitions severely constrain the helicity amplitudes as explained later on. Also, at q^2_{max}, the mesonic current transitions are likely to be strongly influenced by the effects of current-meson intermediate states. Such meson-dominated current transitions are not likely to match up with the point-like current transitions of the free quark decay amplitudes.

For $q^2 = 0$ the FQD amplitude $h_o'^{FQD}$ vanishes. In matching the helicity amplitudes of FQD and mesonic transitions one has to remember to include the $1/\sqrt{2}$ factors of the triplet and singlet spin wave functions of the $(b\bar{q}_{spectator})$ and $(c\bar{q}_{spectator})$ meson bound states. One obtains

$$\frac{1}{2}\, h_0^{FQD} \simeq I \cdot H_0^{D} \simeq I \cdot H_0^{D^*}$$
$$\frac{1}{\sqrt{2}}\, h_{\mp}^{FQD} \simeq I \cdot H_{\mp}^{D^*} \qquad (4)$$

We have introduced the proportionality factor I which will later be identified with the wave function overlap integral between the two mesons involved in the current transition.

Then by identifying $m_b = M_B$ and $m_c = M_D$ ($\simeq M_{D^*}$) we obtain

$$F_{+(0)}^{V} = I,$$
$$F_{1(0)}^{A} = (M_1+M_2) \cdot I,$$
$$F_{2(0)}^{A} = -2/(M_1+M_2) \cdot I \qquad (5)$$
$$F_{(0)}^{V} = -2/(M_1+M_2) \cdot I$$

from comparing (2) and (3) at $q^2 = 0$.*)

It is clear that the proportionality factor in Eq.(4) and (5) has to be identified with the wave function overlap factor I, since in the equal mass limit with no mismatch, charge normalization requires I = 1. Also the same mismatch factor appears in B → D and B → D* since D and D* have the same spatial properties in the quark model. In the unequal mass situation $m_b \gg m_c$ one expects incomplete overlap between the B and D(D*) wave functions leading to I < 1. This is due to the fact that the light spectator quark's low momentum does not match with the energetic c-quark coming from the weak b → c decay when they are collected in the D(D*) wave function. In order to be definite we take I = 0.7 for the wave function overlap mismatch factor I as e.g. estimated in [4] for the b → c transitions.

*) The solution (5) covers the semileptonic transitions $\bar{B}^0 \to D^+(D^{*+})$ and $B^- \to D^0(D^{*0})$. For semileptonic decays involving the quark transition $\bar{b} \to \bar{c} + \ell^+ + \nu_\ell$ the matching solutions are the same for $F_+^V(0)$, $F_1^A(0)$, $F_2^A(0)$ but involve an extra minus sign for $F^V(0)$. This leads to $H_+ \leftrightarrow H_-$ as Eq.(3) shows.

The q^2-dependence of the form factors is fixed by nearest meson-dominance in the appropriate current channel with monopole behaviour (q^{-2}) for F_+^V and F_1^A and dipole behaviour (q^{-4}) for F_2^A and F^V according to the power-counting rules of QCD [14]. For the sake of simplicity we work only with one effective meson ($b\bar{c}$) current mass, for which we take B_c^* (6.34 GeV). The spacing among the various ($b\bar{c}$) bound state levels is presumably so small that one effective mass value is sufficient to set the scale of the q^2-dependence in the range $0 \leq q^2 \leq (M_1-M_2)^2$.

The q^2-dependence of our form factors is thus given by

$$F(q^2) = F(0) \left(\frac{m_{FF}^2}{m_{FF}^2 - q^2} \right)^n \qquad (6)$$

where n = 1 for F_+^V and F_1^A, n = 2 for F_2^A and F^V and m_{FF} = 6.34 GeV.

The matching solutions (5) and the power-behaved form factors (6) completely specify our model of B → D(D*) semileptonic decays.*) For brevity's sake we shall in the following refer to this model as the KS (Körner-Schuler) model.

Except for the above choice of value of the overlap mismatch factor I this model of semileptonic B-decays has already been written down in [13] using, however, a closed form covariant derivation of the matching equations (4).

In order to provide a connection with the work of [13] (see also [10]) we shall briefly outline the covariant deviation of the matching solutions (5) as given in [10,13]. We boost the rest frame quark model wave functions to their respective moving frames. This can be done covariantly by writing covariant quark model wave functions as in [15]:

*) Identical q^2=0 form factor values have been used in [4] following from an infinite momentum frame analysis. However, the authors of Ref.[4] use monpole type form factors also for the higher momentum form factors F_2^A and F^V in disagreement with the power counting rules.

$$J^{PC} = 0^{-+} : M_A{}^B = (\gamma_5(\not P - M)_\alpha{}^\beta M_a{}^b$$
$$J^{PC} = 1^{--} : M_A{}^B = (\not\epsilon(\not P - M))_\alpha{}^\beta M_a{}^b \qquad (7)$$

where $A \equiv (\alpha,a)$ ($B \equiv (\beta,b)$) denote the spinor and flavour indices of the quark (antiquark). P and M are the momentum and mass of the meson and $M_a{}^b$ are the usual flavour wave functions of the mesons.

The above form factor structure Eq.(5) can then be obtained in closed form by computing the traces

$$\langle D(P_2)|V_\mu|B(P_1)\rangle = \frac{1}{M_1+M_2}\ \mathrm{Tr}(\gamma_5(\not P_1 - M_1)\gamma_\mu\gamma_5(\not P_2+M_2)) \qquad (8a)$$

$$\langle D^*(p_2)|V_\mu+A_\mu|B(p_1)\rangle = \frac{1}{M_1+M_2}\ \mathrm{Tr}(\gamma_5(\not P_1 - M_1)\gamma_\mu(1-\gamma_5)\not\epsilon_2(\not P_2+M_2)) \qquad (8b)$$

at $q^2=0$. We have not explicitly written out the flavour traces $M_{1a}{}^b V_b{}^c \bar M_{2c}{}^a$ and $M_{1a}{}^b A_b{}^c M_{2c}{}^a$ in (8) which are simply given by the KM matrix element V_{bc}. We have introduced the overall normalization factor $(M_1+M_2)^{-1}$ in (8) such that (8a) has the correct charge normalization at $q^2=0$.

Let us now turn to the semileptonic decay distributions. The double differential decay distribution for $B\to D^*(D) + \ell^-+\bar\nu_\ell$ is given by (in units of $|V_{bc}|^2$) *) **)

$$\frac{d\Gamma}{dq^2 dE_\ell} = \frac{G^2}{(2\pi)^3}\frac{1}{16}\frac{q^2}{M_1^2}\left((1-\cos\Theta)^2\,|H_-|^2 + (1+\cos\Theta)^2\,|H_+|^2 + 2(1-\cos^2\Theta)\,|H_o|^2\right) \qquad (9)$$

where Θ is the polar angle between the D(D*) and the lepton ℓ^- in the $(\ell^-\bar\nu_\ell)$ CM system, and where

$$2M_1\, p\cos\Theta = M_1^2 - M_2^2 + q^2 - 4M_1 E_\ell \ . \qquad (10)$$

*) When using Eq.(9) and (11) for free quark decay one must remember to include the statistical factor 1/2 in the differential decay distribution.

**) For semileptonic decays involving the quark transition $\bar b\to\bar c + \ell^+ + \nu_\ell$ one has to exchange the transverse helicity contributions in Eq.(9) $|H_+|^2 \leftrightarrow |H_-|^2$.

The E_ℓ (or cosΘ) integration of (9) can be done trivially and results in the differential q^2-distribution (in units of $|V_{bc}|^2$)

$$\frac{d\Gamma}{dq^2} = \frac{G^2}{(2\pi)^3}\frac{q^2 p}{12M_1^2}\left(|H_-|^2 + |H_+|^2 + |H_o|^2\right) \qquad (11)$$

In Fig.1b we have plotted our predictions for the differential q^2-distribution for $B\to D(D^*) + \ell^- + \bar\nu_\ell$ including a separation of the longitudinal and transverse (+) and (-) contributions.

One notes that $d\Gamma_o^D/dq^2 = d\Gamma_o^{D^*}/dq^2$ at $q^2=0$ as is clear from the spin matching argument (4). A pseudothreshold ($q^2=q^2_{max}$) the $B\to D$ transition shows p-wave behaviour ($\sim (q^2-q^2_{max})^{3/2}$) and the $B\to D^*$ transition s-wave behaviour ($\sim (q^2-q^2_{max})^{1/2}$) with $|H_-^{D^*}|^2 = |H_+^{D^*}|^2 = |H_o^{D^*}|^2$.

In Fig.1a we have also plotted the q^2-distribution according to free quark decay using $m_b = 4.73$ GeV and $m_c = 1.55$ GeV. At pseudothreshold the free quark decay is s-wave dominated ($\sim (q^2-q^2_{max})^{1/2}$) with $|h_o^{FQD}|^2 = |h_o'^{FQD}|^2 = \frac{1}{2}|h_-^{FQD}|^2 = \frac{1}{2}|h_+^{FQD}|^2$ leading to equal contributions of the longitudinal and both transverse currents at pseudothreshold. From comparing Fig.1a and 1b one can see that the p-wave pseudothreshold behaviour of the $B\to D$ transition can never be modelled by the s-wave dominated free quark decay when one is close to q^2_{max}. This causes noproblem for the $B\to D^*$ transitions which are s-wave dominated as is the free quark decay. The fact that $|H_+^{D^*}|^2 < |H_-^{D^*}|^2$ and $|h_+^{FQD}|^2 < |h_-^{FQD}|^2$ away from pseudothreshold reflects the chirality structure of the $b\to c$ transition.

In Table 1 we list our predictions for the q^2-integrated rates. For the ratio $r = \Gamma^{D^*}/(\Gamma^{D^*}+\Gamma^D)$ we find $r = 0.78$ which is compatible with the experimental value $r = 0.85 \pm 0.32$ [16]. In fact, it is quite unavoidable that $r > 0.5$ in the spectator quark model. The threshold behaviour at $q^2 = q^2_{max}$ and slope values at $q^2 = 0$ of the longitudinal contributions imply

$\Gamma_o^{D^*} > \Gamma_o^D$ such that $r > 0.5$. Models that feature $r > 0.5$ [11] must be judged to be incompatible with the spectator quark model. For the ratio Γ^{D^*}/Γ^D we find 3.1 which is close to the "magical" ratio 3 which would follow from a naive counting of the spin degrees of freedom. Note though, that the ratio $\simeq 3$ in our approach is a consequence of quark dynamics and not due to spin counting as shown by the fact that the helicity states of the D* are populated quite differently. That $\Gamma^{D^*} \simeq 3\Gamma^D$ has also recently been argued for on very general grounds by Shifman and Voloshin in Ref.[21].

From (4) and (5) (including the statistical spin factor $1/(2S+1)$ in the free quark decay) it is clear that for $I = 1$ and no q^2-dependence in the form factors one expects $\Gamma^{FQM}_{s.\ell.} \simeq \Gamma^D_{s.\ell.} + \Gamma^{D^*}_{s.\ell.}$. Table 1 shows that we indeed predict $\Gamma^{FQM}_{s.\ell.} \simeq \Gamma^D_{s.\ell.} + \Gamma^{D^*}_{s.\ell.}$ which shows that the suppression $I = 0.7$ due to momentum mismatch and the time-like form factor enhancement tend to compensate each other. Therefore we predict that the D and D* exclusive modes constitute a large fraction of the total semileptonic rate.

Numerically we find $\Gamma^{D+D^*}_{s.\ell.}/\Gamma_{total} = 7.8 \times (I/0.7)^2\%$ for $V_{cb} = 0.045$ [17] and $\Gamma^{exp}_{total} \simeq 0.88 \times 10^{12}\ sec^{-1}$ [19], as compared to the total experimental semileptonic branching fraction $\simeq 11.8\%$ [20]. It is clear that the above estimate of 7.8% is subject to change when either the experimental measurements of V_{cb} and the B life-time change, or when the theoretical estimate of the overlap mismatch factor I changes as has been indicated above.

In Fig.2 we show the Dalitz plot for $\bar{B}^o \to D^{*+} + \ell^- + \bar{\nu}_\ell$. Matching of the spectator quark model and the invariant form factors in our approach are done in region I ($q^2 \simeq 0$). This is also the region where the transition form factors are needed in the factorization approach to the nonleptonic B-decays [12,13] involving the $b \to c$ transition as indicated on the q^2-axis. Other authors prefer the pseudothreshold region II ($q^2 \simeq (M_1-M_2)^2$) for the matching procedure [10,11] where the D*(D) is produced at rest.

From Eq.(3) one notes that the transformation between the $B \to D^*$ helicity amplitudes (which are amenable to a quark model calculation) and the invariant amplitudes becomes singular at pseudothreshold $q^2 = (M_1-M_2)^2$ where the D*'s momentum p goes to zero. If one evaluates the quark model amplitudes at this point it is clear that information on the higher momentum form factors F^V and F_2^A is lost unless one evaluates relativistic $O(p/M_{D^*})$ corrections to the static quark model.

In the approach of [6] only the static quark model limit was evaluated and thus no information was obtained on the form factors F^V and F_2^A which are set to zero. This is similar to the models of Ref.[2] and [12] which also feature $F^V = F_2^A = 0$. As is evident from Eq.(3) this results in the loss of chirality information, i.e. in these models $d\Gamma^{D^*}_+/dq^2 = d\Gamma^{D^*}_-/dq^2$ as is apparent from Fig.1d.

The authors of Ref.[5] expanded their quark model results to first order in (p/M_{D^*}) and thus they were able to calculate F^V but not F_2^A which they set to zero.*) We show their q^2-distribution in Fig.1c. The inclusion of the form factor F^V now leads to the correct chiral property $d\Gamma_+/dq^2 \leq d\Gamma_-/dq^2$ as is expected from the underlying left-chiral $b \to c$ quark transition. However, the omission of the higher order form factor F_2^A is not justified close to $q^2 = 0$ as is evident from Eq.(3). In both the GIW [5] and PS [6] models the neglect of the F_2^A contribution leads to an unreasonably large enhancement of the D* channel at $q^2 \sim 0$ compared to the D channel, which, as we have argued above, is in disagreement with the spectator quark model approach.

---

*) The predictions of the nonrelativistic quark model become progressively less reliable as one attempts to include higher order relativistic corrections. Altomari and Wolfenstein [9] expand their quark model calculation to second order in (p/M_{D^*}) and thus obtain an approximate value for F_2^A at $q^2 \sim (M_1-M_2)^2$ which, quite remarkably, is in approximate agreement with our model results.

On the other hand, extrapolating our form factors to $q^2 = q^2_{max}$ we find qualitative agreement with the results of [5,6] for the lower (momentum) order form factors F^+, F_1^A and F^V (in the case of [5]). It seems safer to extrapolate quark model results into the singular region than out of it. Note also, that our matching procedure is done far away from the problematic quark and particle pseudothreshold region.

The difference among the three models clearly show up in the q^2-integrated rates of Table 1. Whereas all three models are in approximate agreement for the transverse $B \to D^*$ contributions (except for PS on Γ_{T+}) there is a marked difference in the predictions for the longitudinal $B \to D^*$ contribution. This also shows up in the predictions for the total $B \to D^*$ semileptonic rates which is large for the GIW model and quite large for the PS model. These large $B \to D^*$ rates result solely from an overestimate of the longitudinal contribution. As argued above this is due to having (erraneously) neglected the contribution of the higher momentum form factor F_2^A. This point is emphasized when one compares the longitudinal/transverse contributions of the GIW and PS models with the free quark decay model in Table 1. It is quite clear that the use of the GIW and PS models to extract values of V_{bc} from experimental data would lead to an underestimate of V_{cb} as has also been stressed in Ref.[9].

For the $B \to D$ semileptonic rates the PS and KS models agree, whereas GIW obtain a larger rate. The GIW prediction for the Γ^{D^*}/Γ^D ratio is 3.5 and close to our prediction of 3.1, whereas the PS prediction is quite large at 9.6. Concerning the ratio $r = (\Gamma^{D^*}+\Gamma^D)/\Gamma^{D^*}$ all three models are compatible with the experimental measurement $r = 0.85 \pm 0.32$ [16].

It would be very useful if experimentalists could check on the helicity patterns predicted by the various models as drawn in Fig.1b-1d and listed in Table 1. The helicity pattern could be checked by either analyzing the

angular decay distributions of the weak decay $W^-_{virtual} \to \ell^- + \bar{\nu}_\ell$ and/or the strong decay $D^* \to D\pi$.

The polar angle distribution of the weak decay $W^-_{virtual} \to \ell^- + \bar{\nu}_\ell$ is already contained in Eq.(9) and provides a unique opportunity to check on the handedness of the $b \to c$ transition, which, for the canonical (V-A) form, leads to $|H_+^{D^*}|^2 < |H_-^{D^*}|^2$ for $q^2 < q^2_{max}$ regardless of the details of the underlying quark dynamics. Such an angular measurement constitutes a true $\langle \vec{p}\vec{S} \rangle$ p.v. type measurement of the handedness of the $b \to c$ transition. Attempts to conclude for the $b \to c$ handedness solely from the shape of the lepton energy endpoint spectrum (which is p.c. observable) are much more problematic because of their model dependence.

On the other hand, the angular distribution of the strong decay $D^* \to D\pi$ is only sensitive to the sum of the transverse contributions and the longitudinal contribution. For the angular decay distribution one finds

$$W(\cos\Theta^*) = 1 + \alpha \cos^2\Theta^* \qquad (12)$$

where Θ^* is the polar angle of the D (or π) in the D^* rest frame relative to the D^* momentum direction. In terms of the $B \to D^*$ helicity amplitudes the asymmetry parameter α reads

$$\alpha = \frac{2|H_0^{D^*}|^2 - |H_+^{D^*}|^2 - |H_-^{D^*}|^2}{|H_+^{D^*}|^2 + |H_-^{D^*}|^2} \qquad (13)$$

Our predictions for the asymmetry value α are listed in Table 1, together with those of the GIW and PS models. Our calculation gives the smallest value for the asymmetry parameter ($\alpha = 1.06$), and the PS model the largest value ($\alpha = 5.38$).

The CLEO collaboration have recently reported on a measurement of the asymmetry parameter [18], albeit in the restricted phase space region

$1.2\ \text{GeV} \leq E_{\ell^-} \leq E_{\ell^-}(\text{max})$ and $\cos\Phi'(\ell,\pi) < -0.7$, where $\Phi'(\ell,\pi)$ is the angle between ℓ^- and π. In Fig.3 we have plotted the dependence of the asymmetry parameter α on the lower lepton energy cut-off. Assuming that the above angle cut is not stringent we can compare the predictions of the three models with the measurement of Ref.[18]. For $E_\ell(\text{lower}) = 1.2$ GeV we find $\alpha^{-1} = 1.61$ (KS), 0.42 (GIW) and 0.22 (PS). The CLEO collaboration quotes $\alpha^{-1} < 0.33$ at 90% CL suggesting dominance of the longitudinal contribution as is also the case for the GIW and PS models. However, this agreement is fortuitous since the dominance of the longitudinal contribution in the GIW and PS models is a consequence of having neglected the contribution of the second order form factor F_2^A. As already argued above, this neglect leads to unreasonably large longitudinal contributions in semileptonic $B \to D^*$ transitions which is in disagreement with the spectator model close to $q^2=0$. Our value of $\alpha^{-1} = 1.61$ is in disagreement with the measurement [18]. It implies approximate equality of longitudinal and transverse contributions ($\Gamma_L = 0.82\ \Gamma_T$). Let us stress that anything but approximate equality or dominance of the transverse over the longitudinal contribution for lower energy cut values $E_\ell(\text{lower}) \geq 1.2$ GeV would be very hard to accommodate theoretically if one believes in the spectator quark model approach. In order to settle this issue it would be very important to have an independent confirmation of the CLEO measurement.

Let us mention that an additional check on the transverse/longitudinal helicity composition of the $B \to D^*$ transition can be obtained from nonleptonic B-decays involving a $b \to c$ transition. Within the factorization approximation [12,13] the nonleptonic decays involve the same transition form factors as the semileptonic decays. Thus an analysis of the angular decay distributions in $D^* \to D\pi$ and/or $\rho \to \pi\pi$ following the weak decay $B \to D^*\rho$ would provide the opportunity to obtain information on the transverse/longitudinal composition of the $B \to D^*$ transition at a fixed low value of $q^2 = m_\rho^2$. Note that

the predictions of the three models differ most for such small q^2-values. A similar statement holds for the decay $B \to D^*f^*$ for the higher fixed value of $q^2=m_{f^*}^2$. Note that the decay $B \to D^*f^*$ is expected to have a substantial branching ratio [13].

We now turn to the differential lepton energy distributions which are obtained from (9) by q^2-integration in the interval

$$0 \leq q^2 \leq 2E_\ell \frac{M_1^2-M_2^2-2M_1E_\ell}{(M_1-2E_\ell)} .$$

In Fig.4 we show the E_ℓ-spectra for free quark decay, our spectator model, the GIW model [5] and the PS model [6] including again a separation of the various helicity contributions.

As is apparent from comparing the different spectra in Fig.4 the shapes of the GIW and PS spectra are qualitatively different from the FQD and KS spectra. Adding up the two longitudinal contributions $\Gamma_L^{D^*}$ and Γ^D to facilitate the comparison with the FQD spectra one finds qualitative agreement between the KS and FQD spectra, whereas the GIW and PS spectra differ from the FQD spectra particularly in the endpoint region.

A nice qualitative discussion of the shape of the endpoint spectrum is afforded by an expansion of the differential energy distribution around $E_\ell(\text{max}) = (M_1^2-M_2^2)/2M_1$ in powers of $(E_\ell(\text{max}) - E_\ell)$.

For the longitudinal contributions one obtains

$$\frac{d\Gamma_o^{D,D^*}}{dE_\ell} \sim \frac{G^2}{16\pi^3}\frac{1}{M_2^2}\,4\,|\sqrt{q^2}\,H_{o(0)}^{D,D^*}|^2\,(E_\ell(\text{max}) - E_\ell)^2 \qquad (14)$$

and for the transverse contributions

$$\frac{d\Gamma_-^{D^*}}{dE_\ell} \sim \frac{G^2}{16\pi^3}\,\frac{(M_1^2-M_2^2)^2}{M_2^4}\,|H_{-(0)}^{D^*}|^2\,(E_\ell(\text{max}) - E_\ell)^2 \qquad (15)$$

$$\frac{d\Gamma_+^{D^*}}{dE_\ell} \sim \frac{G^2}{16\pi^3}\frac{2}{3}\,\frac{M_1^2}{M_2^4(M_1^2-M_2^2)}\,|H_{+(0)}^{D^*}|^2\,(E_\ell(max)-E_\ell)^4 \qquad (16)$$

The chirally suppressed transverse (+) contribution vanishes with the fourth power at the kinematic boundary, whereas the longitudinal and transverse (-) contributions vanish with the second power.*) The corresponding FQD behaviour is simply obtained by substituting the corresponding $q^2 = 0$ FQD helicity amplitudes $h_o^{FQD}(0)$, $h_-^{FQD}(0)$ and $h_+^{FQD}(0)$ and by multiplying the statistical factor $1/(2S+1) = 1/2$.

From an inspection of the endpoint region in Fig.4 one notes that the transverse (-) distribution dominates the endpoint spectrum in the FQD and KS models. In fact, comparing Eqs.(14), (15) and (3-5) one finds to leading order in $(M_1/M_2)^2$

$$d\Gamma_-/d\Gamma_L = \frac{1}{2}\left(\frac{M_1}{M_2}\right)^2\left(1+O\left(\left(\frac{M_1}{M_2}\right)^2\right)\right) \qquad (17)$$

in the KS and FQD models. Here we have again taken the sum of the $B \to D$ and longitudinal $B \to D^*$ contributions in $d\Gamma_L$ in order to be able to compare the FQD and KS models. As Eq.(17) shows explicitly, the transverse (-) contribution dominates the endpoint spectrum for the FQD and KS models.

The present discussion implies also that the decay distribution $D^* \to D\pi$ should be dominantly transverse for large lepton energies. This observation highlights the puzzle posed by the experimental observation of the CLEO collaboration that the $D^* \to D\pi$ decay distributions is dominated by the longitudinal contribution for medium and large lepton energies [18].

*) At the lower bound $E_\ell = 0$ the role of the transverse (+) and (-) contributions are exchanged: the transverse (-) contribution behaves as E_ℓ^4 and the transverse (+) and longitudinal contributions as E_ℓ^2.

A corresponding analysis of the endpoint region in the GIW model shows that the transverse (-) contribution is not as dominating as in the FQD and KS models as is evident from Fig.4d. In the case of the PS model one finds $d\Gamma_-^{D^*}/d\Gamma_L^{D^*} \sim 1$ and $d\Gamma_-^{D^*}/d\Gamma_L^{D} \sim (M_1/M_2)^2$ which implies that the transverse (-) and longitudinal contributions of $B \to D^*$ contribute equally in the endpoint region as is also evident from Fig.4d.

From this discussion of the shape of the lepton energy spectrum in the endpoint region, which is determined by the $q^2 = 0$ behaviour of the transition form factors, it is clear that it is dangerous to rely on quark models that are reliable only in a q^2-region far away from $q^2 = 0$ (as is the case for the GIW and PS models) when discussing the lepton energy endpoint spectrum.

In Fig.5 we show our prediction for the q^2-spectra of the $b \to u$ semileptonic decays $\bar{B}^o \to \rho^+ + \ell^- + \bar{\nu}_\ell$ and $\bar{B}^o \to \pi^+ + \ell^- + \bar{\nu}_\ell$ including a separation of the transverse and longitudinal contributions in the case of $B \to \rho$. The mismatch in the momentum of the spectator quark and the energetic u-quark from b decay is more pronounced and we expect $I_{B\to\pi(\rho)} \ll I_{B\to D(D^*)}$. For definiteness we take $I_{B\to\pi(\rho)} = 0.33$ as estimated in Ref.[4]. For the meson entering the meson dominance form factors (6) we take the $J^{PC} = 1^{--}$ bottom meson which is expected to have a mass of $m_{B^*} = 5.33$ GeV.

From Fig.5 one notes that the predicted q^2-spectra of semileptonic $B \to \rho$ decays are more weighted towards the large q^2-values than their $B \to D^*$ counter-parts in Fig.1b. This is in part due to the fact that the form factor enhancement towards q^2_{max} is quite substantial in this case. The form factor variation from $q^2 = 0$ to $q^2_{max} = (M_1-M_2)^2$ is 3.52 (14.3 in the case of $B \to \pi$) for the monopole type form factor and 12.4 for the dipole type form factor in Eq.(6). This large enhancement rate also explains the dominance of the transverse (-) contribution in the $B \to \rho$ case as Fig.5 shows.

For the integrated exclusive semileptonic rates we obtain

$$\bar{B}^0 \to \pi^- : \Gamma_{s.\ell.} = 7.25\ |V_{bu}|^2\ 10^{12}\ \text{sec}^{-1}$$
$$\bar{B}^0 \to \rho^- : \Gamma_{s.\ell.} = 33.0\ |V_{bu}|^2\ 10^{12}\ \text{sec}^{-1} \qquad (17)$$

with

$$\Gamma_- : L : \Gamma_+ = 0.62 : 0.33 : 0.05 \qquad (18)$$

for the longitudinal/transverse composition in the latter case.*)

The predicted semileptonic $B \to \pi$ rate essentially agrees with the prediction of [4], but is larger by a factor of 3.5 than the GIW prediction [5]. For $B \to \rho$ we obtain larger semileptonic rates than [4] which is due to the fact that we use dipole form factors for F_2^A and F^V as dictated by the power counting rules instead of the monopole form factors used in [4]. Both our model and the model of [4] yield larger semileptonic $B \to \rho$ rates than GIW [5].

In conclusion we have presented detailed predictions of a spectator quark model for exclusive semileptonic B-decays which emphasizes the similarity between exclusive B-decays and the free b-quark decay in the small q^2-region. The small q^2-region is appropriate for a matching of the two descriptions since it is far away from the problematic pseudothreshold region where the particles spins enter nontrivially through (pseudo) threshold constraints. A correct description of the small q^2-region is crucial for the correct description of the lepton energy endpoint spectrum and for the calculation of nonleptonic rates via the factorization approach. The main theoretical uncertainty concerns the theoretical value for the wave function overlap mismatch factor I which affects our predictions for the total exclusive semileptonic rates. This theoretical uncertainty, however, does not affect our predictions for the relative semileptonic $B \to D^*$ rates, the shapes of the q^2 and lepton energy spectra and the longitudinal transverse helicity composition of the semileptonic decays.

*) The semileptonic rates for $\bar{B}^- \to \pi^0(\rho^0)$ are down by a factor of 2 compared to the rates (17) as can be easily seen in the quark model approach.

References

[1] S. Behrends et al. (CLEO Collaboration), Phys.Rev.Lett. 59(1987)407;
G. Levman et al. (CUSB Collaboration), Phys.Lett. 141B(1984)271;
S. Weseler (ARGUS Collaboration), Ph.D. Thesis, Univ. of Heidelberg, April 1986, IHEP-HD/86-2;
H. Albrecht et al. (ARGUS Collaboration), DESY preprint 87-079;
K. Wachs (Crystal Ball Collaboration), DESY preprint 87-084

[2] A. Ali, Z.Physik C1(1979)25

[3] G. Altarelli et al., Nucl.Phys. B208(1982)365

[4] M. Wirbel, B. Stech and M. Bauer, Z.Phys. C29(1985)637

[5] B. Grinstein, M.B. Wise and N. Isgur, Phys.Rev.Lett. 56(1986)298 and CALTECH preprint CALT-68-1311 (1986)

[6] F. Schöberl and H. Pietschmann, Europhys.Lett. 2(1986)583

[7] J.G. Körner in "Proceedings of the International Symposium on Production and Decay of Heavy Hadrons", Heidelberg 1986

[8] S. Nussinov and W. Wetzel, Phys.Rev. D36(1987)130

[9] T. Altomari and L. Wolfenstein, Phys.Rev.Lett. 58(1987)1583 and Carnegie-Mellon preprint CMU-HEP-86-17

[10] M. Suzuki, Nucl.Phys. B258(1985)553

[11] S. Chao, R. Kass, G. Kramer, W. Palmer and S. Pinsky, Phys.Rev. D31(1985)1756

[12] D. Fakirov and B. Stech, Nucl.Phys. B133(1978)315

[13] A. Ali, J.G. Körner, G. Kramer and J. Willrodt, Z.Phys. C1(1979)269

[14] S.J. Brodsky and G.P. Lepage, Phys.Rev. D22(1980)2157

[15] R. Delbourgo, A. Salam and J. Strathdee, Proc.Roy.Soc. A278(1965)146;
T. Gudehus, Phys.Rev. 184(1969)1788

[16] A. Chen et al. (CLEO Collaboration), Phys.Rev.Lett. 52(1984)1084;
E.H. Thorndike: Weak decays of heavy fermions, published in Proceedings of "International Symposium on Lepton and Photon Interactions", Kyoto 1985

[17] K. Kleinknecht: Central Value for V_{cb} in the Six-Quark Analysis, Comments Nucl.Part.Phys. 13(1984)219

[18] S. Csorna et al. (CLEO Collaboration), "Observation of D** Meson Polarization in Semileptonic B-Meson Decay", paper Nr.364, submitted to International Symposium on Lepton and Photon Interactions at High Energies, Hamburg 1987.

[19] V. Lüth in Proceedings of the "International Symposium on Production and Decay of Heavy Hadrons", Heidelberg 1986

[20] D.G. Hitlin, "Weak Decays of Heavy Quarks", CALTECH preprint CALT-68-1420

[21] M.A. Shifman and M.B. Voloshin, Moskau ITEP preprint ITEP-87-64

Figure Captions

Fig. 1: Differential q^2-distribution of semileptonic bottom decays $b \to c + \ell^- + \bar{\nu}_\ell$ and $B \to D(D^*) + \ell^- + \bar{\nu}_\ell$, a) free quark decay (FQD), b) spectator model (KS), c) model of Ref.[5] (GIW), d) model of Ref.[6] (PS). Full lines: semileptonic $b \to c$ rate for (a); semileptonic $B \to D^*$ and $B \to D$ rates for (a), (b), (c). Dotted lines: transverse (+) and (-) and longitudinal contributions to $b \to c$ and $B \to D^*$ rates.

Fig. 2: Dalitz plot for $B^0 \to D^{*+} + \ell^- + \bar{\nu}_\ell$. Peak occurs for $q^2 = (M_1-M_2)^2$ and $E_\ell = \frac{1}{2}(M_1-M_2) \cdot E_\ell(\max) = (M_1^2-M_2^2)/2M_1$. Region I and region II (pseudothreshold region) indicate the regions where our and the model of [4], and the models of [5,6,9], respectively, match invariant form factors to quark model results. Arrows on the q^2-axis indicate where form factors are needed for the factorization approach to nonleptonic B-decays involving $b \to c$ transitions.

Fig.3 : Differential lepton energy distribution of semileptonic bottom decays $b \to c + \ell^- + \bar{\nu}_\ell$ and $B \to D(D^*) + \ell^- + \bar{\nu}_\ell$. Explanation as in Fig.1.

Fig. 4: Values of asymmetry parameter α versus lower lepton energy cut $E_\ell(\text{cut})$ for decay $D^* \to D\pi$. Asymmetry parameter determined in the integration region $E_\ell(\text{cut}) \leq E_\ell \leq E_\ell(\max)$.

Fig. 5: Differential q^2-distribution for semileptonic bottom decays $\bar{B}^0 \to \rho^+ + \ell^- + \bar{\nu}_\ell$ and $\bar{B}^0 \to \pi^+ + \ell^- + \bar{\nu}_\ell$. Explanation of full and dotted lines given in Fig.1.

	Γ_{T-}	Γ_{T+}	Γ_L	$\Gamma_{T+L}^{B\to D^*}$	Γ_{T+L}	$\frac{\Gamma^{D^*}}{\Gamma^D}$	$r = \frac{\Gamma^{D^*}}{\Gamma^D+\Gamma^{D^*}}$	α
	$[\lvert V_{bc}\rvert^2 \times 10^{12}\ \text{sec}^{-1}]$							
FQD	10.0	2.4	24.8	-	37.1	-	-	-
Mode								
KS	9.8	B→D* 2.9	B→D* 13.1	B→D 8.3	B→D* 25.8	B→D*+D* 34.1	3.1	0.76	B→D* 1.06
GIW[5]	11.6	3.0	35.0	14.3	49.6	63.9	3.5	0.78	3.83
PS[6]	8.2	8.2	52.4	7.2	68.8	76.0	9.6	0.91	5.38

Table 1: Semileptonic decay rates involving a $b \to c$ transition. First row: Free quark decay (FQD) $b \to c + \ell^- + \bar{\nu}_\ell$. Row 3-5: $B^0 \to D^+(D^{*+}) + \ell^- + \bar{\nu}_\ell$ decays in our spectator quark model approach (KS), and in the quark models of Grinstein, Isgur, Wise (GIW) and Pietschmann, Schöberl (PS). Listed are transverse/longitudinal (T/L) helicity compositions of the semileptonic rates. Also shown are ratios of $B \to D^*$ and $B \to D$ rates, as well as the asymmetry parameter α for the strong decay $D^* \to D\pi$.

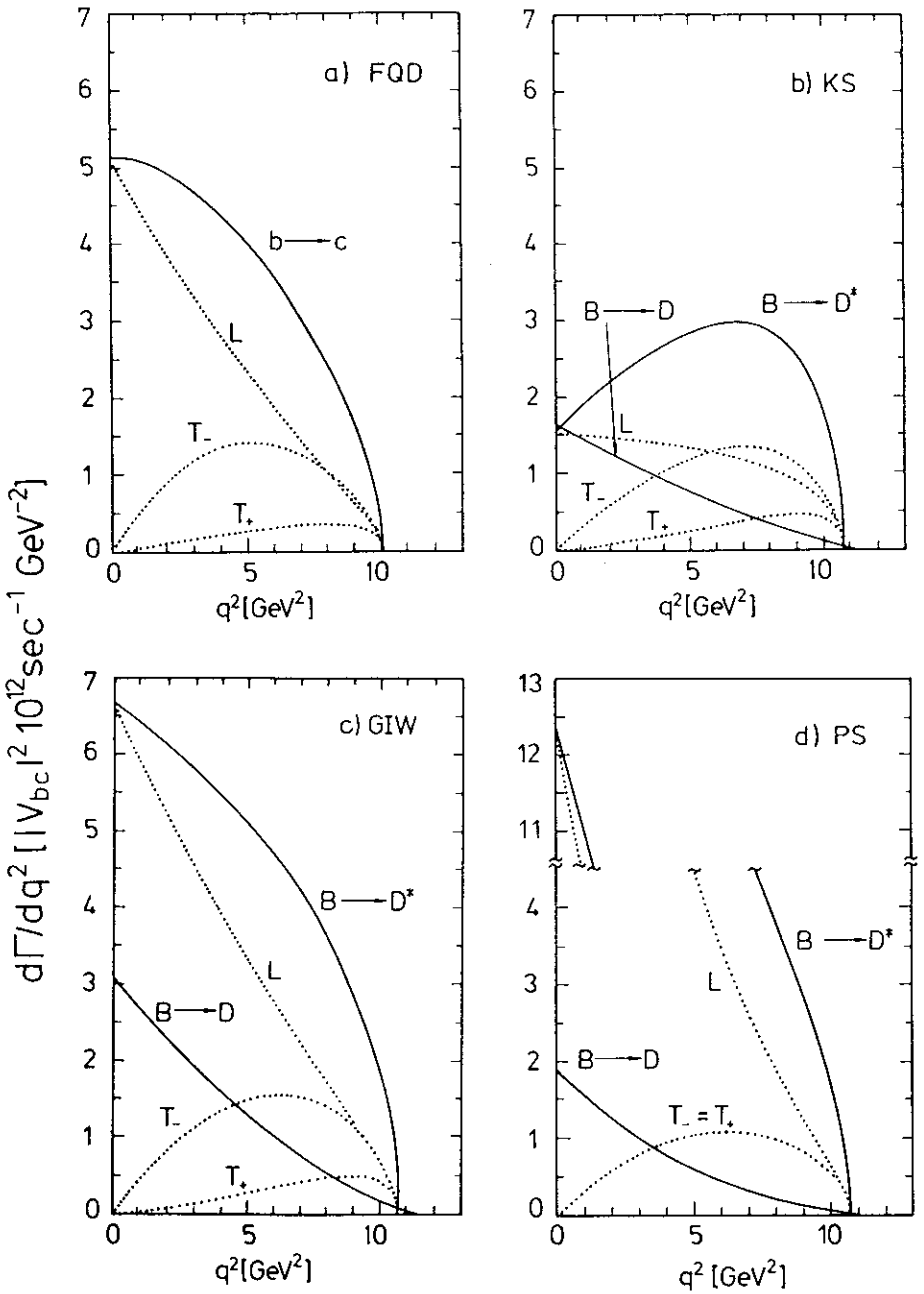
a) FQD
b) KS
c) GIW
d) PS
b→c
B→D
B→D*
L
T-
T+
T- = T+
dΓ/dq² [|Vbc|² 10¹² sec⁻¹ GeV⁻²]
q² [GeV²]

Fig. 1

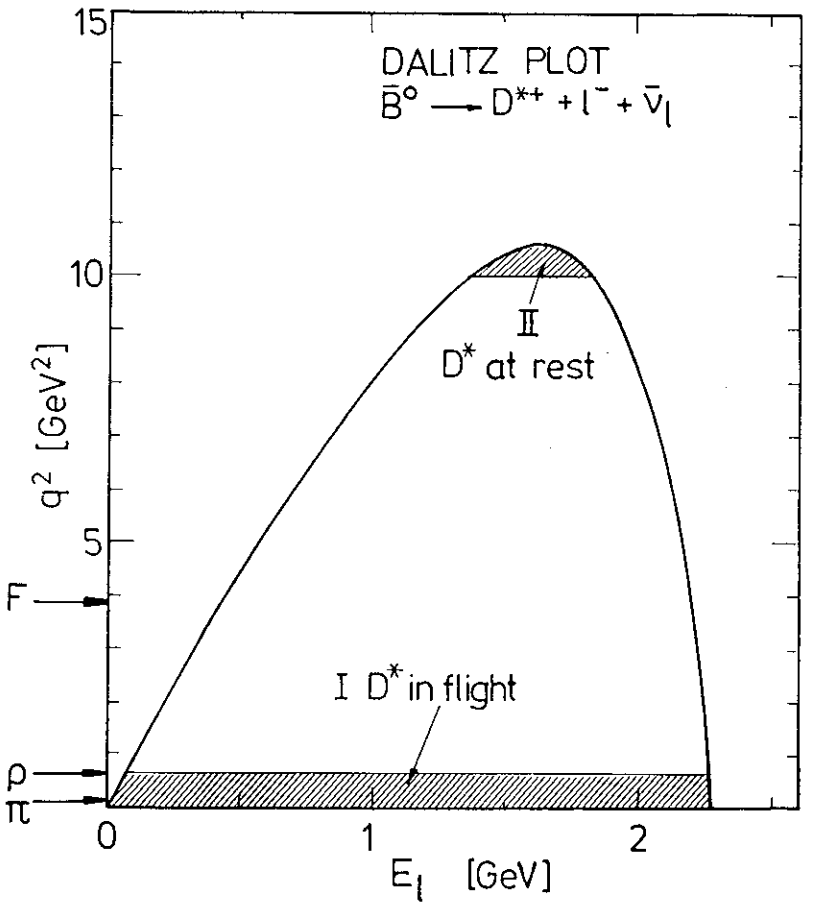
DALITZ PLOT
B̄° → D*+ + l⁻ + ν̄l
q² [GeV²]
II
D* at rest
I D* in flight
F
ρ
π
El [GeV]

Fig. 2

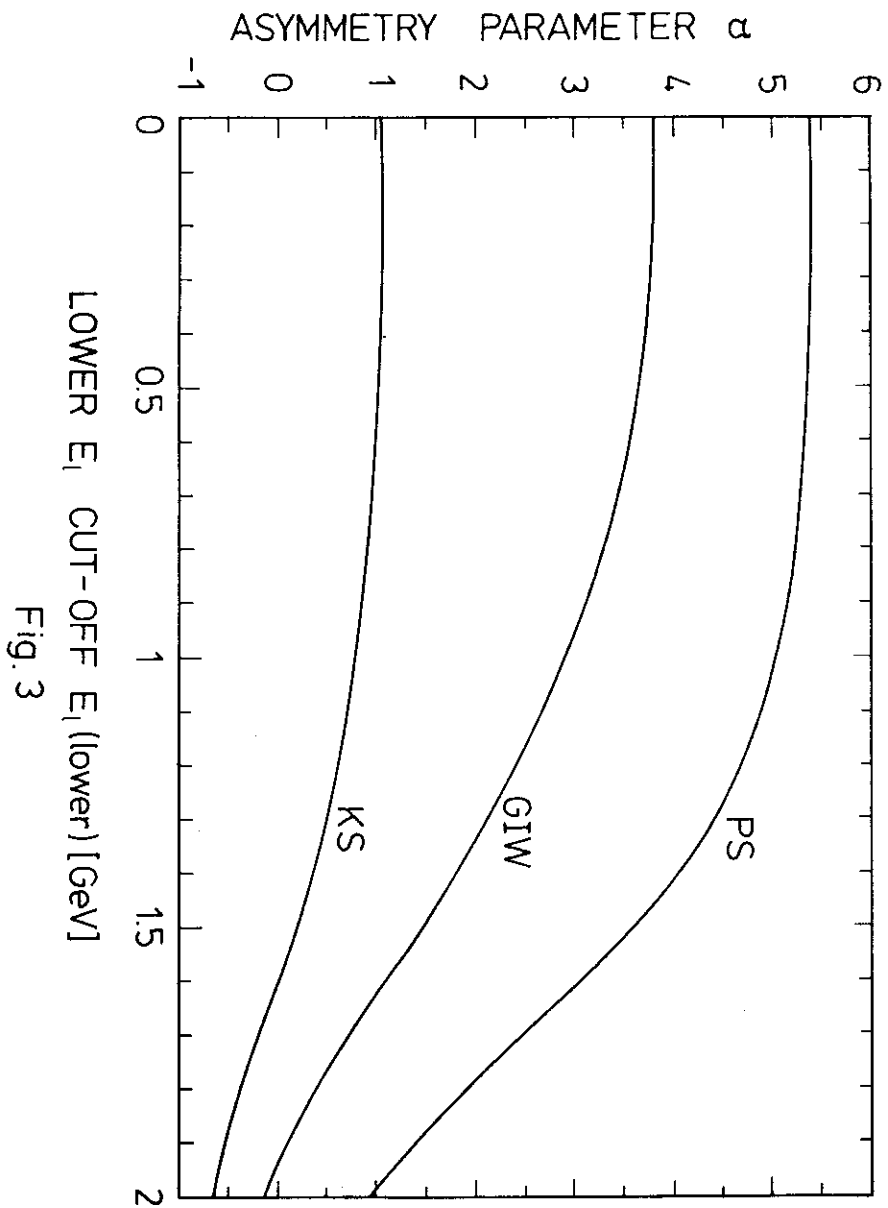
ASYMMETRY PARAMETER α
-1
0
1
2
3
4
5
6
LOWER E_l CUT-OFF E_l (lower) [GeV]
0
0.5
1
1.5
2
KS
GIW
PS

Fig. 3

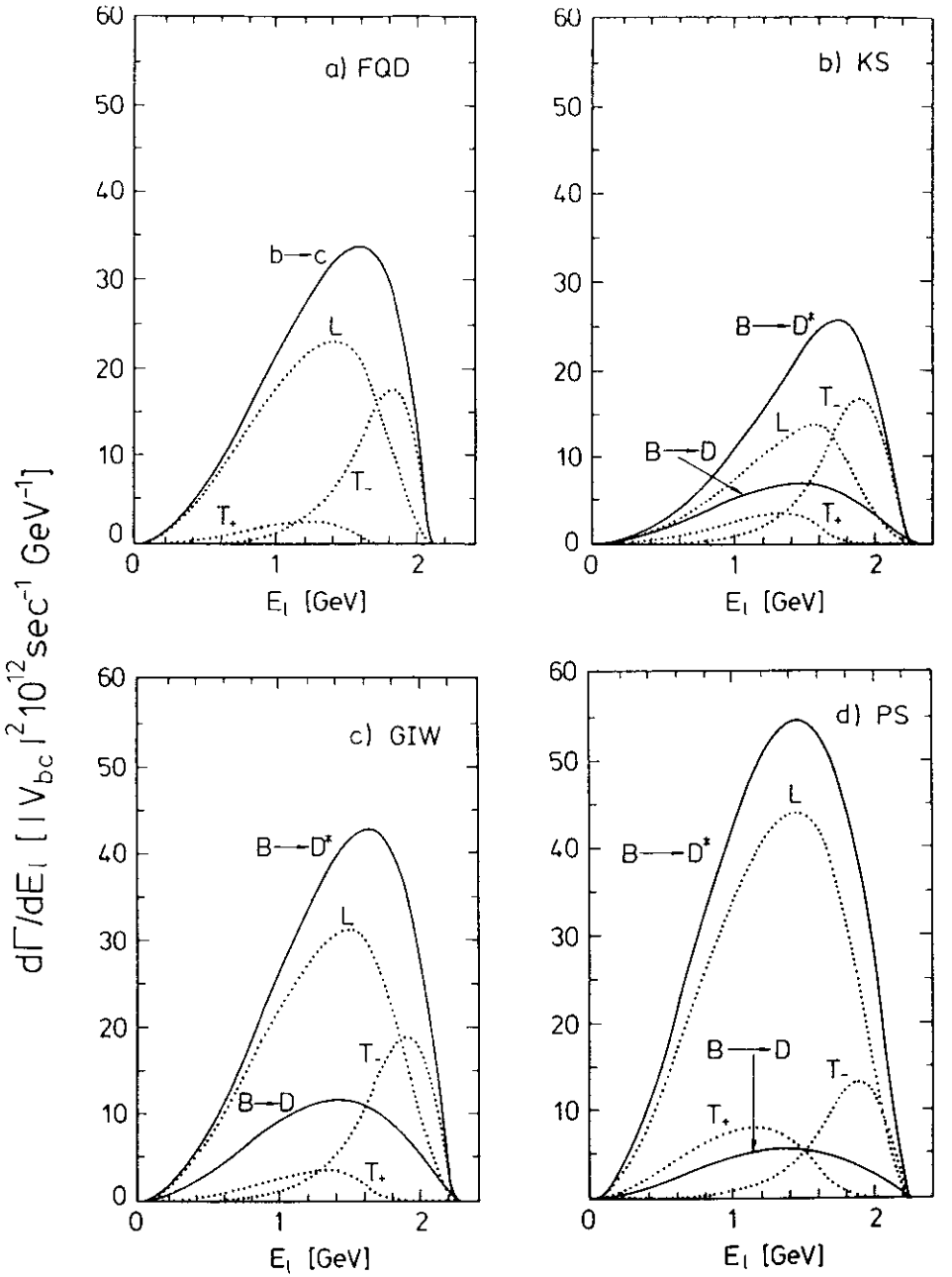
a) FQD
b) KS
c) GIW
d) PS
b→c
B→D*
B→D
L
T+
T-
E_l [GeV]
$d\Gamma/dE_l$ [$|V_{bc}|^2 10^{12} sec^{-1} GeV^{-1}$]

Fig. 4

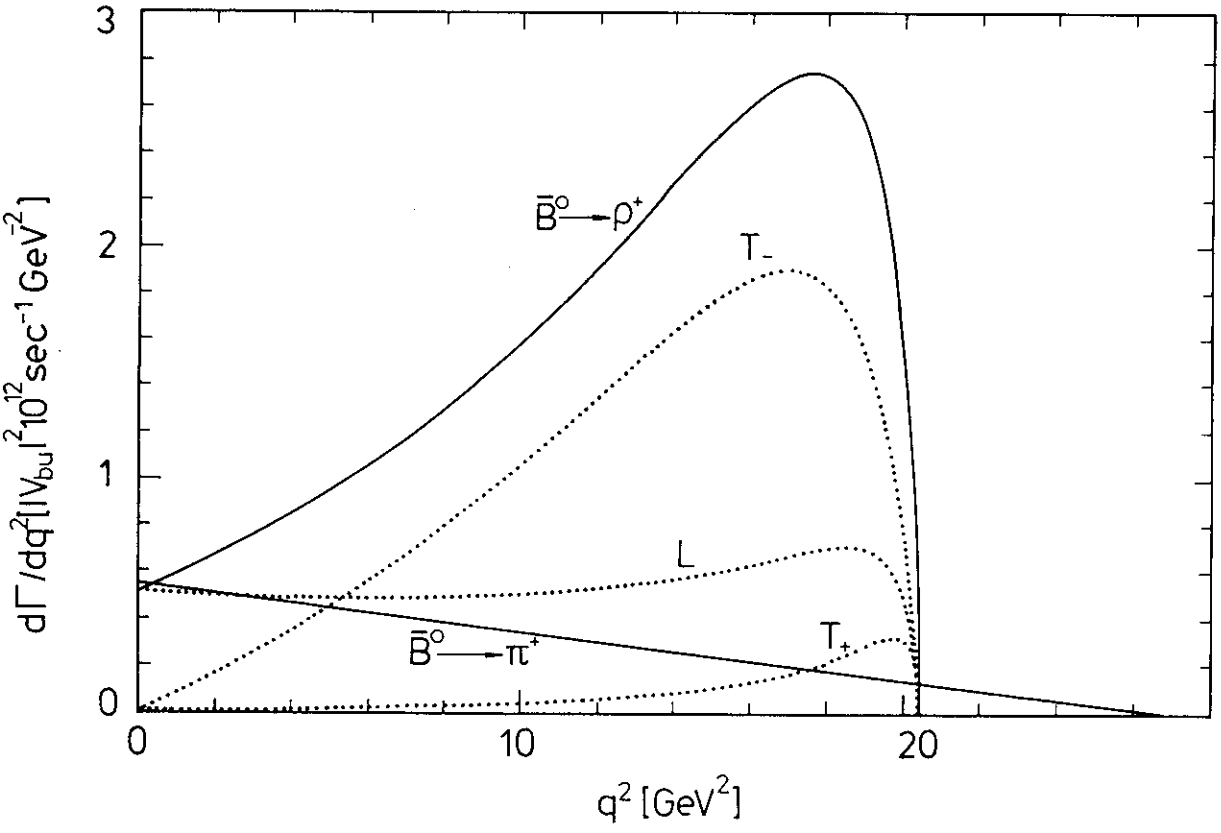
3
2
1
0
0
10
20
$d\Gamma/dq^2[|V_{bu}|^2 10^{12} sec^{-1} GeV^{-2}]$
q^2 [GeV^2]
$\bar{B}^0 \to \rho^+$
$\bar{B}^0 \to \pi^+$
T-
L
T+

Fig. 5